

Holocene history of the Larsen-A Ice Shelf constrained by geomagnetic paleointensity dating

Stefanie Brachfeld* Byrd Polar Research Center, Ohio State University, Columbus, Ohio 43210, USA

Eugene Domack Department of Geology, Hamilton College, Clinton, New York 13323, USA

Catherine Kissel } Laboratoire des Sciences du Climat et de l'Environnement, Unite mixte Commissariat à l'Energie Atomique
Carlo Laj } et Centre National de la Recherche Scientifique, Gif-sur-Yvette, France

Amy Leventer Department of Geology, Colgate University, Hamilton, New York 13346, USA

Scott Ishman Department of Geology, Southern Illinois University, Carbondale, Illinois 62901, USA

Robert Gilbert Department of Geography, Queen's University, Kingston, Ontario K7L 3N6, Canada

Angelo Camerlenghi Istituto Nazionale di Oceanografia e di Geofisica Sperimentale, Trieste, Italy

Lorraine B. Eglinton Department of Marine Chemistry and Geochemistry, Woods Hole Oceanographic Institution, Woods Hole, Massachusetts 02543, USA

ABSTRACT

A sedimentary record collected from beneath the former Larsen-A Ice Shelf reveals the Holocene history of the Larsen-A region. The record begins with the transition from grounded ice to a floating ice shelf, completed by 10.7 ± 0.5 ka, and ends with the modern recession. The record contains several late Holocene diatomaceous ooze layers that suggest proximity to productive open-water events. Radiocarbon ages obtained from these sediments were complicated by the presence of detrital and reworked carbon. We have eliminated these complications and constructed a chronology for the Larsen-A Ice Shelf history via tuning of the geomagnetic field paleointensity record with a reference curve. This approach provides chronological control to sediment sequences that lack appropriate material for radiocarbon dating. Geomagnetic paleointensity features with wavelengths of 2–3 k.y. can be recognized and interhemispherically correlated, illustrating the potential to use geomagnetic paleointensity variations as a global correlation and dating tool at sub-Milankovitch time scales.

Keywords: Larsen Ice Shelf, Antarctic Peninsula, geomagnetic paleointensity, Holocene.

INTRODUCTION

Public attention has been focused on the Antarctic Peninsula due to the rapid disintegration of the northern and middle sections of the Larsen Ice Shelf (LIS-A and LIS-B, respectively) (Rott et al., 1996; Vaughan and Doake, 1996; De Angelis and Skvarca, 2003). The warming trend on the Antarctic Peninsula has pushed the temperature limit of ice shelf viability southward, likely contributing to recent break-up events (Scambos et al., 2001). Melting and calving of ice shelves on both sides of the Antarctica Peninsula have long raised concerns about the future ice-mass flux of the continental tributary glaciers that feed into the ice shelves (Mercer, 1978).

Sediment cores recovered from beneath the former LIS-A contain diatomaceous ooze layers (Fig. 1), suggesting proximity to open-water productive events (Domack et al., 2001a). Radiocarbon dating these Holocene–late Pleistocene Antarctic shelf sediments involves several challenges. Antarctic marine carbonates have an ocean reservoir age of ca. 1200–1300 ^{14}C yr B.P. (Gordon and Harkness, 1992; Harden et al., 1992; Berkman and Forman, 1996). However, much of the sediment accumulating on the Antarctic shelf lacks calcareous organisms, necessitating the use of acid-insoluble organic matter (AIOM) from bulk sediment. The AIOM may be affected by reworked carbon from detrital humic macerals, kerogen from sedimentary rocks, and resus-

pending marine organic matter (Andrews et al., 1999; Domack et al., 1999).

Microscope observations indicate that LIS-A organic carbon is a mixture of ~25% carbon formed and deposited contemporaneously with the sediment and ~75% reworked organic carbon characterized by preaged terrestrial detritus. We obtained a radiocarbon age of 9720 ± 65 ^{14}C yr from a sediment-water interface sample of AIOM and an age of 1010 ± 30 ^{14}C yr from a sample of living bryozoan calcite, which indicates the magnitude (~8700 yr) of the effect of reworked carbon on our radiocarbon ages (Fig. 1; Table 1). However, the surface sediment contains a greater abundance of sterols ($0.3\text{--}0.55$ $\mu\text{g/g}$) than the downcore material (<0.15 $\mu\text{g/g}$), where reworked carbon has had a greater impact on the resultant ages. A regional AIOM correction factor of ~9000–9400 yr is indicated by paired calcite and AIOM ^{14}C ages from LIS-B, where biogenic calcite is much more abundant than in LIS-A (Domack et al., 2002). These observations illustrate the difficulty of relying solely on AIOM radiocarbon ages from organically lean sediment.

Records of high-frequency (<10 k.y.) geomagnetic field paleointensity variations can serve as a global, millennial-scale correlation and dating tool (Channell et al., 2000; Laj et al., 2000; Stoner et al., 2002). Here we demonstrate the utility of geomagnetic field paleointensity as a dating tool for Holocene sediment via tuning with an independently dated reference curve. Our absolute intensity reference curve (denoted ABSINT) is a compilation of more than 2000 absolute paleointensity determinations made on archaeological baked clays (pottery, bricks) and recent volcanic samples from around the world (Yang et al., 2000; Laj et al., 2002) that permits us to import the ^{14}C , K/Ar, and historical absolute ages of ABSINT's samples to the Antarctic margin.

STUDY AREA AND PALEOENVIRONMENTAL PROXIES

Multibeam swath bathymetry (Fig. 1) revealed the 1000-m-deep Greenpeace Trough under the former LIS-A (Domack et al., 2001a). Several sediment cores were collected from the Greenpeace Trough; all display a consistent stratigraphy (Fig. 1). This study focuses on kasten core 23 (KC23: $64^{\circ}47.144'$ S, $60^{\circ}21.566'$ W, 901 m water depth), which contains a complete Holocene stratigraphy. KC23 contains three lithological units (Fig. 2). Unit 1 (0–130 cm) consists of a silty-clay with a minor component of sand and scattered gravel. The upper 3–5 cm of Unit 1a contains unsupported ^{210}Pb , indicative of modern sediment accumulation (Gilbert and Domack, 2003). Unit 2 (130–150 cm) consists of a coarse-grained granulated facies, which represents an ice-proximal water-laid till. Unit 3 (150–230 cm) consists of a structureless black mud with elevated shear strength, which represents a comminution till deposited under grounded ice (Domack et al., 2001a).

*Present address: Department of Earth and Planetary Sciences, Montclair State University, Upper Montclair, New Jersey 07043, USA.

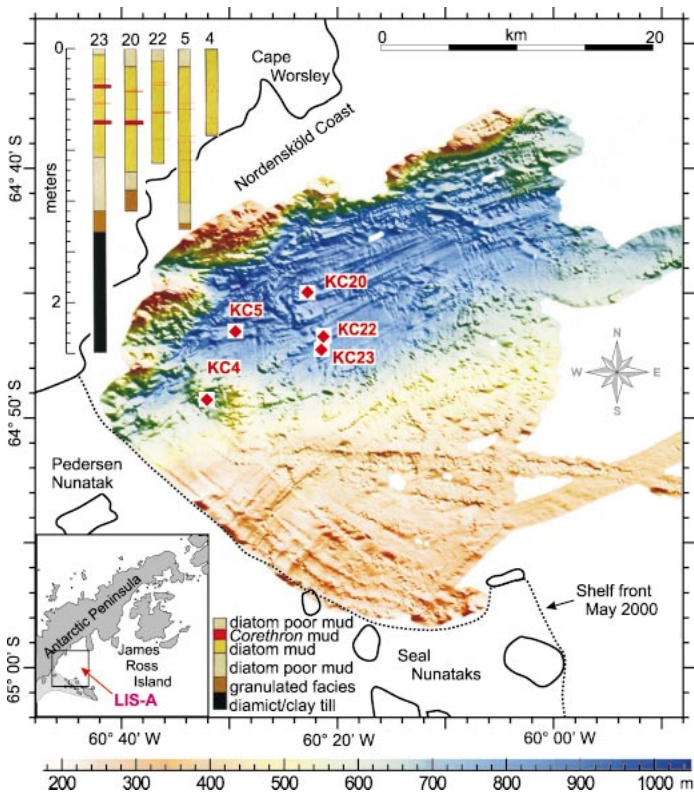


Figure 1. Greenpeace Trough bathymetry, sediment core locations, and generalized lithostratigraphy. Inset: Regional setting of former Larsen-A Ice Shelf (LIS-A).

Foraminiferal faunas are restricted to Unit 1, which contains planktonic, calcareous benthic, and agglutinated taxa. *Neogloboquadrina pachyderma* and calcareous benthic foraminifera are restricted to the upper 10 cm of the core. Arenaceous benthics including *Miliammina* spp. dominate the foraminiferal assemblages down to 122 cm depth (Fig. 2). The arenaceous assemblages represent cold, saline

TABLE 1. RADIOCARBON DATES FROM GREENPEACE TROUGH

Lab No.	Core	Depth (cm)	Uncorrected (^{14}C yr B.P.)	$\delta^{13}\text{C}$	Carbon source
AA49352	G4	0	1010 \pm 30	0.8	Calcite
AA44757	KC5	0–4	9720 \pm 70	–24.2	AIOM
AA44758	KC5	38–40	10,830 \pm 70	–23.7	AIOM
AA44759	KC5	115–117	18,200 \pm 120	–24.2	AIOM
AA44755	KC4	32–34	11,390 \pm 60	–23.2	AIOM
AA44756	KC4	70–72	18,220 \pm 130	–25.0	AIOM
NO28021	KC23	31–33	11,000 \pm 85	–23.9	AIOM
NO28021	KC23	67–70	11,200 \pm 100	–24.9	AIOM
NO28020	KC20	64–65	11,850 \pm 70	–24.1	AIOM

Note: AA = Arizona Accelerator Mass Spectrometry Laboratory; NO = National Ocean Sciences Accelerator Mass Spectrometry Facility; KC = kasten core; G = Smith-McIntyre grab sampler; AIOM = acid-insoluble organic matter. See Figure 1 for sediment core lithostratigraphy.

bottom-water conditions (Milam and Anderson, 1981). The abundance of calcareous planktonic and benthic foraminifera at 0–2 cm indicates an increase in benthic productivity, possibly associated with increased phytoplankton productivity and carbon flux to the seafloor due to the retreat of the LIS-A (Ishman and Szymcek, 2003).

Unit 1 contains three diatomaceous ooze layers (Figs. 1 and 2). These layers contain abundant *Corethron criophilum*, a species that is rarely preserved in Antarctic sediments. The valves are poorly preserved; spines and girdle bands are more common than whole valves. These layers also contain *Fragilariopsis curta*, indicative of sea ice and/or ice edge productivity, and *Thalassiosira gracilis*, a species often associated with a well-mixed water column (Leventer et al., 1996). Uncorrected radiocarbon dates from these layers in KC23 and nearby cores KC4, KC5, and KC20 range from 11,000 to 11,850 ^{14}C yr B.P., in part reflecting contamination with reworked carbon (Fig. 1; Table 1).

GEOMAGNETIC PALEOINTENSITY CHRONOLOGY

Unit 1 sediments record a stable single component of remanence carried by magnetite. Maximum angular deviation values are $<2^\circ$. The inclinations in Unit 1 fluctuate within 15° of the site-specific International Geomagnetic Reference Field value (-57°) (Fig. 3). Below 130

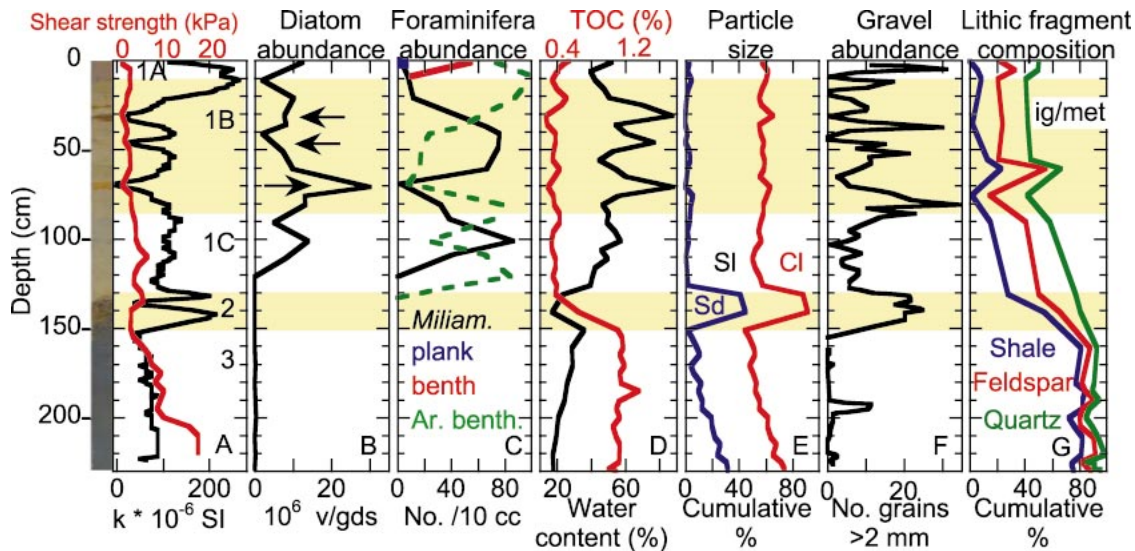


Figure 2. Digital photograph of KC23 and downcore profiles. A: Magnetic susceptibility and shear strength. B: Millions of diatom valves per gram of dry sediment. Arrows denote *Corethron* ooze layers. C: Foraminifera per 20 cm^3 sediment. *Miliammina* spp. (*Milam.*) and arenaceous benthics (*Ar. benth.*) dominate KC23 profile. Calcareous benthics (benth) and planktics (plank) are restricted to Unit 1a. D: Total organic carbon (TOC) and water content. *Corethron* layers have very low TOC content and elevated water content. E: Percentages of sand (Sd), silt (Si), and clay (Cl). F: Gravel grain abundance. G: Lithic fragment composition. Cumulative percent quartz, feldspar, shale, and crystalline igneous and metamorphic rocks (ig/met).

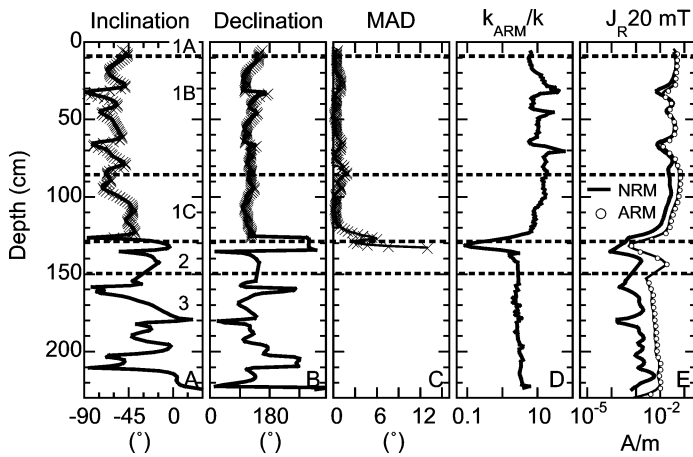


Figure 3. Paleomagnetic data. U-channels were demagnetized and measured on 2G-755R cryogenic magnetometer with in-line alternating field demagnetization system housed at Laboratoire des Sciences du Climat et de l'Environnement, Gif-sur-Yvette, France. A: Inclination. B: Declination. C: Maximum angular deviation (MAD) values. D: Susceptibility of anhysteretic remanent magnetization (ARM) normalized by magnetic susceptibility (k_{ARM}/k), which tracks relative variations in magnetic particle size. E: Intensity of remanence (J_r) after cleaning in 20 mT alternating field. Solid line denotes $\text{NRM}_{20 \text{ mT}}$ (natural remanent magnetization). Open circles denote $\text{ARM}_{20 \text{ mT}}$ (every fourth data point plotted). Steep inclinations within *Corethron* ooze layers are likely measurement artifacts resulting from abrupt changes in lithology. Solid lines in A–E denote data from 20 mT demagnetization level. Principal component analysis (denoted X) was performed using data from 20–50 mT demagnetization levels. Unit 1 sediments record single component of remanence with MAD values $<2^\circ$. Parameter k_{ARM}/k is relatively constant, excluding *Corethron* ooze layers, where extremely weak k biases ratio. Only Unit 1 is suitable for paleointensity analysis.

cm there is no stable direction due to the sediment texture and glaciogenic origin of Units 2 and 3, the latter of which contains pyrrhotite in black shale lithic fragments. Therefore, Units 2 and 3 are inappropriate for paleomagnetic analyses.

We normalized the natural remanent magnetization (NRM) of Unit 1 using two methods based on anhysteretic remanent magnetization (ARM). The first method is the traditional NRM/ARM normalization using NRM and ARM intensities after alternating field (AF) demagnetization at the 20 mT level. The second method calculates relative paleointensity by integrating the area under the NRM and ARM AF demagnetization curves over a given demagnetizing field range (denoted H_{AF} , 20–50 mT in this study), and normalizing according to:

$$\frac{\int_{20 \text{ mT}}^{50 \text{ mT}} \text{NRM}(H_{\text{AF}}) dH_{\text{AF}}}{\int_{20 \text{ mT}}^{50 \text{ mT}} \text{ARM}(H_{\text{AF}}) dH_{\text{AF}}} \quad (1)$$

The two methods yield nearly identical curves (Fig. 4).

The KC23 record is remarkably similar to ABSINT, displaying the broad paleointensity high from 3 to 1 ka, preceded by the relative low from 7.5 to 5 ka. Paleointensity records from the North and South Atlantic Ocean, Indian Ocean, and Greenland ice cores demonstrate that millennial-scale dipole features with wavelengths of 5 k.y. to the very rapid 1 k.y. Laschamp event can be correlated over large areas (Baumgartner et al., 1998; Laj et al., 2000; Wagner et al., 2000; Mazaud et al., 2002; Stoner et al., 2002). The record from KC23 demonstrates that features as brief as 2–3 k.y. can be correlated. The KC23 record was tuned to ABSINT using Analyseries software (Paillard et

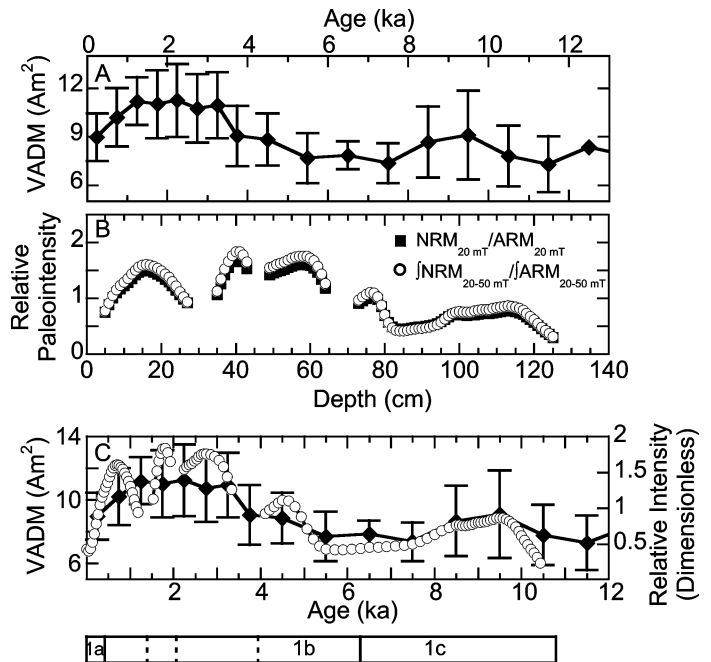


Figure 4. Geomagnetic paleointensity tuning. A: ABSINT (absolute intensity reference curve) virtual apparent dipole moment (VADM) curve (Yang et al., 2000; Laj et al., 2002). B: Normalized relative paleointensity curves from KC23. Solid squares denote $\text{NRM}_{20 \text{ mT}}/\text{ARM}_{20 \text{ mT}}$. Open circles denote integral method. Gaps in record are locations of *Corethron* ooze layers. C: KC23 paleointensity record tuned to ABSINT.

al., 1996), which transfers the ABSINT chronology to the Antarctic margin.

The paleointensity age uncertainties are given by the half-widths of the ABSINT bins, which are 0.5 k.y. for the early to middle Holocene and 0.25 k.y. for the late Holocene. Instrumental analytical errors reported for radiocarbon dates are typically ± 40 –100 yr for organic-rich sediment (total organic carbon $>1\%$) (Andrews et al., 1999; Domack et al., 1999). However, the laboratory counting errors do not reflect the more serious issues of sediment reworking, changing reservoir ages back through time, and spatial and temporal variations in detrital and allochthonous carbon input, all of which may lead to age uncertainties >500 yr (Andrews et al., 1999; Domack et al., 1999).

The paleointensity-based chronology eliminates these complications and enables us to establish the timing of events in the history of LIS-A. The progression from the comminution till and gravelly mud of Units 3 and 2 into the diatomaceous mud of Unit 1 likely represents the Last Glacial Maximum to Holocene transition in the northwestern Weddell Sea. This is manifested as a transition from a grounded ice sheet to a floating ice shelf, as evidenced by shifting gravel provenance from in situ black shale to crystalline igneous and metamorphic rocks derived from further afield. This transition was completed by ca. 10.7 ± 0.5 ka. The transition from Unit 1c to the more diatomaceous Unit 1b is dated as 6.3 ± 0.5 ka, which coincides with the maximum warming and maximum biological productivity observed in records from the western Antarctic Peninsula (Domack et al., 2001b).

The three diatomaceous ooze layers are dated as 1.4 ± 0.25 ka, 2.1 ± 0.25 ka, and 3.8 ± 0.5 ka. The precise mechanisms of formation and emplacement of these layers remain uncertain. However, they occurred after the peak in middle Holocene warming documented on the Antarctic Peninsula (Domack et al., 2001b) and slightly later than other episodes of ice shelf decay in the Antarctic. Sedimentary records from beneath the smaller and more northerly Prince Gustav Ice Shelf suggest that the ice shelf decayed ca. 5–2 ka (Pudsey and Evans, 2001). Re-

cords from the East Antarctic margin indicate both advances and retreats of glaciers ca. 7–1 ka (Domack et al., 1991; Hemer and Harris, 2003). It is likely that the discrepancies in the timing of these events are due to challenges associated with the derivation of an appropriate correction factor to account for marine radiocarbon reservoir variations and the variable input of reworked carbon: hence the appeal of the paleointensity method.

The transition from Unit 1b to the gray, less biogenic Unit 1a is dated as 0.45 ± 0.25 ka. This unit coincides with decreased productivity and cooling observed on the western Antarctic Peninsula (Domack et al., 2001b). The top (0–2 cm) of Unit 1a is characterized by the first appearance of calcareous planktonic foraminifera and increases in calcareous benthic foraminifera and diatom abundance, which marks the modern recession of the ice shelf.

CONCLUSIONS

A sedimentary record from beneath the former LIS-A indicates that the transition from grounded ice to floating ice shelf was completed by ca. 10.7 ± 0.5 ka. The LIS-A was stable throughout the early Holocene. The first suggestion of instability is manifested as a sequence of late Holocene diatomaceous ooze layers, although their origin is still under investigation. We developed a geomagnetic paleointensity-based chronology for KC23 that eliminates complications arising from the lack of datable material and uncertainties arising from the presence of reworked carbon. The similarities between KC23 and ABSINT suggest that geomagnetic field features with wavelengths of 2–3 k.y. can be used for long-range correlation. This supports the suggestion that synchronization between sedimentary paleointensity records and ice-core records of geomagnetically modulated ^{10}Be and ^{36}Cl flux can be used as a millennial-scale correlation and dating tool (Baumgartner et al., 1998; Laj et al., 2000; Wagner et al., 2000; Stoner et al., 2002).

ACKNOWLEDGMENTS

We thank the crew of the *N.B. Palmer*, Raytheon Polar Services, and the Antarctic Research Facility for their efforts during cruise NBP00–03. J. Hayes provided measurements of sterol content and helpful comments. J. Ridge and D. DeMaster provided thorough and thoughtful reviews. This work was supported by National Science Foundation grants OPP-981438, OPP-0003633, INT-0129155, and European Community Grant EVK2-2000-2267.

REFERENCES CITED

Andrews, J.T., Domack, E.W., Cunningham, W.L., Leventer, A., Licht, K.J., Jull, A.J.T., DeMaster, D.J., and Jennings, A.E., 1999, Problems and possible solutions concerning radiocarbon dating of surface marine sediments, Ross Sea, Antarctica: *Quaternary Research*, v. 52, p. 206–216.

Baumgartner, S., Beer, J., Masarik, J., Wagner, G., Meynadier, L., and Synal, H.-A., 1998, Geomagnetic modulation of the ^{36}Cl flux in the GRIP ice core, Greenland: *Science*, v. 279, p. 1330–1332.

Berkman, P.A., and Forman, S.L., 1996, Pre-bomb radiocarbon and the reservoir correction for calcareous marine species in the Southern Ocean: *Geophysical Research Letters*, v. 23, p. 363–366.

Channell, J.E.T., Stoner, J.S., Hodell, D.A., and Charles, C.D., 2000, Geomagnetic paleointensity for the last 100 kyr from the sub-Antarctic South Atlantic: A tool for interhemispheric correlation: *Earth and Planetary Science Letters*, v. 175, p. 145–160.

De Angelis, H., and Skvarca, P., 2003, Glacier surge after ice shelf collapse: *Science*, v. 299, p. 1560–1562.

Domack, E.W., Jull, A.J.T., and Nakao, S., 1991, Advance of East Antarctic outlet glaciers during the hypsithermal: Implications for the volume state of the Antarctic ice sheet under global warming: *Geology*, v. 19, p. 1059–1062.

Domack, E.W., Jacobson, E.A., Shipp, S., and Anderson, J.B., 1999, Late Pleistocene–Holocene retreat of the West Antarctic Ice Sheet system in the Ross Sea: Part 2—Sedimentologic and stratigraphic signature: *Geological Society of America Bulletin*, v. 111, p. 1517–1536.

Domack, E.W., Leventer, A., Gilbert, R., Brachfeld, S., Ishman, S., Camerlenghi, A., Gavahan, K., Carlson, D., and Barkoukis, A., 2001a, Cruise reveals history of Holocene Larsen Ice Shelf: *Eos (Transactions, American Geophysical Union)*, v. 82, p. 13, 16–17.

Domack, E.W., Leventer, A., Dunbar, R., Taylor, F., Brachfeld, S., Sjunneskog, C., and the ODP Leg 178 Scientific Party, 2001b, Chronology of the

Palmer Deep site, Antarctic Peninsula: A Holocene palaeoenvironmental reference for the circum-Antarctic: *Holocene*, v. 11, p. 1–9.

Domack, E.W., Duran, D., McMullen, K., Gilbert, R., and Leventer, A., 2002, Sediment lithofacies from beneath the Larsen B Ice Shelf: Can we detect ice shelf fluctuation?: *Eos (Transactions, American Geophysical Union)*, v. 83, p. F301.

Gilbert, R., and Domack, E.W., 2003, The sedimentary record of disintegrating ice shelves in a warming climate, Antarctic Peninsula: *Geochemistry, Geophysics, Geosystems*, v. 4, 1038 doi:10.2929/2002GC000441.

Gordon, J.E., and Harkness, D.D., 1992, Magnitude and geographic variation of the radiocarbon content in Antarctic marine life: Implications for reservoir corrections in radiocarbon dating: *Quaternary Science Reviews*, v. 11, p. 696–708.

Harden, S.L., DeMaster, D.J., and Nittrouer, C.A., 1992, Developing sediment geochronologies for high-latitude continental shelf deposits: A radiochemical approach: *Marine Geology*, v. 103, p. 69–97.

Hemer, M.A., and Harris, P.T., 2003, Sediment core from beneath the Amery Ice Shelf, East Antarctica, suggests mid-Holocene ice-shelf retreat: *Geology*, v. 31, p. 127–130.

Ishman, S.E., and Szymek, P., 2003, Foraminiferal distributions in the former Larsen-A ice shelf and Prince Gustav Channel region, eastern Antarctic Peninsula margin: A baseline for Holocene paleoenvironmental change, in Domack, E.W.D., et al., eds., *Antarctic Peninsula climate variability: A historical and paleoenvironmental perspective: American Geophysical Union Antarctic Research Series* (in press).

Laj, C., Kissel, C., Mazaud, A., Channell, J.E.T., and Beer, J., 2000, North Atlantic paleointensity stack since 75 ka (NAPIS-75) and the duration of the Laschamp event: *Royal Society of London Philosophical Transactions, ser. A*, v. 358, p. 1009–1025.

Laj, C., Kissel, C., Mazaud, A., Michel, E., Muscheler, R., and Beer, J., 2002, Geomagnetic field intensity, North Atlantic Deep Water circulation and atmospheric $\Delta^{14}\text{C}$ during the last 50 kyr: *Earth and Planetary Science Letters*, v. 200, p. 177–190.

Leventer, A., Domack, E.W., Ishman, S., Brachfeld, S., McClennen, C., and Manley, P., 1996, 200–300 year productivity cycles in the Antarctic Peninsula region: Understanding linkages among the sun, atmosphere, oceans, sea ice and biota: *Geological Society of America Bulletin*, v. 108, p. 1626–1644.

Mazaud, A., Sicre, M.A., Ezat, U., Pichon, J.J., Duprat, J., Laj, C., Kissel, C., Beaufort, L., Michel, E., and Turon, J.L., 2002, Geomagnetic-assisted stratigraphy and sea surface temperature changes in core MD94–103 (Southern Indian Ocean): Possible implications for north-south climatic relationships around H4: *Earth and Planetary Science Letters*, v. 201, p. 159–170.

Mercer, J.H., 1978, West Antarctic ice sheet and CO_2 greenhouse effect: A threat of disaster: *Nature*, v. 271, p. 321–325.

Milam, R.W., and Anderson, J.B., 1981, Distribution and ecology of recent benthic foraminifera of the Adélie-George V continental shelf and slope, Antarctica: *Marine Micropaleontology*, v. 6, p. 297–325.

Paillard, D., Labeyrie, L., and Yiou, P., 1996, Macintosh program performs time-series analysis: *Eos (Transactions, American Geophysical Union)*, v. 77, p. 379.

Pudsey, C.J., and Evans, J., 2001, First survey of Antarctic sub-ice shelf sediments reveals mid-Holocene ice shelf retreat: *Geology*, v. 29, p. 787–790.

Rott, H., Skvarca, P., and Nagler, T., 1996, Rapid collapse of Northern Larsen Ice Shelf, Antarctica: *Science*, v. 271, p. 788–792.

Scambos, T.A., Hulbe, C., Fahenstock, M., and Bohlander, J., 2001, The link between climate warming and break-up of ice shelves in the Antarctic Peninsula: *Journal of Glaciology*, v. 154, p. 516–530.

Stoner, J.S., Laj, C., Channell, J.E.T., and Kissel, C., 2002, South Atlantic and North Atlantic geomagnetic paleointensity stacks (0–80 ka): Implications for interhemispheric correlation: *Quaternary Science Reviews*, v. 21, p. 1141–1151.

Vaughan, D.G., and Doake, C.S.M., 1996, Recent atmospheric warming and retreat of ice shelves on the Antarctic Peninsula: *Nature*, v. 379, p. 328–331.

Wagner, G., Masarik, J., Beer, J., Baumgartner, S., Imboden, J.D., Kubik, P.W., Synal, H.A., and Suter, M., 2000, Reconstruction of the geomagnetic field between 20 and 60 kyr BP from cosmogenic radionuclides in the GRIP ice core: *Nuclear Instruments and Methods in Physics Research B*, v. 172, p. 597–604.

Yang, S., Odah, H., and Shaw, J., 2000, Variations in the geomagnetic dipole moment over the last 12,000 years: *Geophysical Journal International*, v. 140, p. 158–162.

Manuscript received 4 March 2003

Revised manuscript received 13 May 2003

Manuscript accepted 15 May 2003

Printed in USA